



Solution NMR studies reveal the location of the second transmembrane domain of the human sigma-1 receptor



Jose Luis Ortega-Roldan*, Felipe Ossa, Nader T. Amin, Jason R. Schnell*

Department of Biochemistry, University of Oxford, South Parks Road, Oxford OX1 3QU, UK

ARTICLE INFO

Article history:

Received 14 November 2014
Revised 19 January 2015
Accepted 22 January 2015
Available online 31 January 2015

Edited by Christian Griesinger

Keywords:

Sigma-1 receptor
Transmembrane domain
NMR

ABSTRACT

The sigma-1 receptor (S1R) is a ligand-regulated membrane chaperone protein associated with endoplasmic reticulum stress response, and modulation of ion channel activities at the plasma membrane. We report here a solution NMR study of a S1R construct (S1R(Δ 35)) in which only the first transmembrane domain and the eight-residue N-terminus have been removed. The second transmembrane helix is found to be composed of residues 91–107, which corresponds to the first steroid binding domain-like region. The cytosolic domain is found to contain three helices, and the secondary structure and backbone dynamics of the chaperone domain are consistent with that determined previously for the chaperone domain alone. The position of TM2 provides a framework for ongoing studies of S1R ligand binding and oligomerisation.

© 2015 The Authors. Published by Elsevier B.V. on behalf of the Federation of European Biochemical Societies. This is an open access article under the CC BY-NC-ND license (<http://creativecommons.org/licenses/by-nc-nd/4.0/>).

1. Introduction

The sigma-1 receptor (S1R) is a membrane chaperone protein present varyingly in both the endoplasmic reticulum (ER) and plasma membranes, where it functions as an accessory protein to a number of ion channels and receptors [1–3]. S1R has been observed to modulate the activity of several ion channels including IP3 receptors [2,4] and voltage-gated channels selective for potassium [5,6], sodium [7], and calcium [8]. S1R has also been shown to interact with acid-sensing ion channels [9], glutamate receptors [10], and dopamine receptors [11]. S1R is highly expressed in the central nervous system (CNS), primarily in the cerebral cortex, hippocampus and cerebellar Purkinje cells [12,13], and binds a large number of small molecules (opiates, antipsychotics, antidepressants, antihistamines, phencyclidine-like compounds, β -adrenergic receptor ligands, cocaine, dimethyltryptamine, progesterone, and sphingosine), many of which have been shown to modulate the effect of S1R on receptors and ion channels (reviewed in [14,15]). Thus, S1R is a potential therapeutic target in the treatment of a range of diseases of the CNS, including schizophrenia, Alzheimer's and Parkinson's diseases, amnesia, depression, amyotrophic lateral sclerosis and addiction.

S1R contains two transmembrane domains connected by a cytosolic domain, and an ER-accessible C-terminal chaperone

domain [1,6]. Based on homology to the steroid binding regions of fungal sterol C7–C8 isomerases, the regions from residues 91–109 and 176–194 have been termed Steroid Binding Domain Like I and II (SBDLI and SBDLII, respectively), and shown by mutagenesis and chemical derivatisation studies to be located within the S1R ligand binding site [16,17].

In addition, several residues immediately N-terminal to SBDLI have been implicated in S1R oligomerisation, including a five amino acid sequence (GGWMG; residues 87–91) proposed to contain a glycoporphin A-like GxxxG intramembrane dimerisation motif [18,19]. S1R oligomerisation is ligand dependent and may provide a mechanism by which its activity is regulated [18,20]. An oligomerisation interface at or near SBDLI would provide an obvious structural link to drug binding.

Whereas SBDLII is centered on helix 3 of the membrane associated chaperone domain [17,21], the structure of the region encompassing SBDLI and its relationship to the membrane is not known. Sequence-based predictions of transmembrane helices indicate that SBDLI will have at least some overlap with the second transmembrane helix (TM2). However, these predictions do not converge on a single position for TM2 (Table 1). Of the algorithms tested, some indicate the presence of a transmembrane helix between residues ~80–100, whereas others locate it between residues ~90–110, and at least one algorithm fails to confidently identify any transmembrane helix in this region.

Because of the importance of SBDLI and the adjacent region in ligand binding and receptor oligomerisation, defining the residues that constitute TM2 can shed light on the structural link between

* Corresponding authors.

E-mail addresses: Jose.Ortega-Roldan@bioch.ox.ac.uk (J.L. Ortega-Roldan), Jason.Schnell@bioch.ox.ac.uk (J.R. Schnell).

these two features of S1R function. We previously showed that the S1R chaperone domain could be reconstituted into DPC detergent micelles as a monomeric species capable of binding the ER chaperone BiP [21]. The S1R chaperone domain was found to contain five helices (H1–H5) and a flexible internal region of ~30 amino acids containing at least two regions with propensity to adopt an extended conformation. The fourth helix in the chaperone domain is amphipathic and likely drives its association with membranes. Here we report solution NMR studies of a novel S1R construct (S1R(Δ 35)) in which the first transmembrane domain has been removed, enabling a description of the residues within the TM2 helix and the secondary structure of the cytosolic domain. We show that the topology and backbone dynamics of natively purified S1R(Δ 35) is consistent with that determined previously for the chaperone domain [21], that TM2 consists of residues 91–107, and that the cytosolic region contains three helices (cH1–cH3). Identification of the TM2 residues provides a framework for further studies of S1R ligand binding and oligomerisation.

2. Materials and methods

2.1. Protein sample production

An ACA-free gene construct (GeneArt) containing an N-terminal (His)₆-tag or a (His)₉-tag, a Factor Xa cleavage site, and residues 36–223 of human S1R was subcloned into the pCOLD-I vector (Takara) and confirmed by sequencing. The substitution C94A, shown to have no effect on ligand binding in full-length guinea pig S1R [17], was introduced to prevent intermolecular disulfide bond formation during purification. The N-terminal sequence preceding the S1R residues 36–223 was MNHKVHHHHHHIEGRHM or MNHKVHHHHHHHHHIEGRHM. The S1R(Δ 35) plasmid and a pMazF plasmid containing the gene for the RNA interferase MazF (Takara) were transformed into C43(DE3) cells. Transformed cells were grown to an OD₆₀₀ of 0.8–0.9, cold shocked on ice, and incubated for 45 min at 15 °C. Cells were pelleted and washed with M9 salt solution, pelleted a second time, and then resuspended into a 10-fold lower volume of isotopically labeled media. Cells were incubated for a further 45–60 min at 15 °C before induction with 2.5 mM IPTG. Expression proceeded for 20 h at 15 °C. Membranes were collected by centrifugation at 200000×g, and incubated overnight in a solution containing 6 M guanidine, 200 mM NaCl, 1% Triton, and 20 mM Tris at pH 8.0. S1R(Δ 35) was separated by Ni affinity chromatography and dialyzed against water to remove guanidine. The precipitated protein was resolubilized in hexafluoro-2-propanol and purified by HPLC on a C3 reverse phase column over a gradient from buffer A (95% water, 5% acetonitrile, 0.1% trifluoroacetic acid) to buffer B (57% 2-propanol, 38%

acetonitrile, 5% water, 0.1% trifluoroacetic acid). Fractions containing S1R(Δ 35) were pooled and lyophilized. For the native purification, the resuspended membranes were incubated overnight with 1% dodecylphosphocholine (DPC). The solubilized membranes were purified by Ni affinity chromatography in 20 mM DPC and subsequently gel filtrated into a low DPC concentration (3.3 mM) in a Superdex200 column (GE). Both methods yielded approximately 40 mg of pure protein per liter of labeled media. The lipid 1,2-dipalmitoyl-sn-glycero-3-phosphocholine (DPPC) was added from powder to the sample to a *q* ratio of 0.1, where $q = [\text{lipid}]/[\text{detergent}]$.

2.2. Circular dichroism

Samples for circular dichroism (CD) contained 12.6 or 7.3 μ M protein of S1R(cd) or S1R(Δ 35), respectively, in DPC:DPPC mixed micelles at a *q* ratio of 0.1, and 20 mM potassium phosphate at pH 6.5. CD spectra were collected at room temperature on a Jasco J-815 circular dichroism spectropolarimeter from 250 to 200 nm with 10 accumulations. Data were smoothed with a Savitsky–Golay filter [22] using a window of 11 points and then corrected for concentration and number of residues.

2.3. NMR spectroscopy and data analysis

NMR experiments for resonance assignments were recorded on ²H, ¹⁵N, and ¹³C labeled samples in DPC:DPPC mixed micelles at a *q* ratio of 0.1, in 20 mM potassium phosphate at pH 6.5. Spectra were recorded at 600 MHz (¹H) on a Bruker Avance III HD spectrometer equipped with a TCI CryoProbe at 41 °C. Backbone resonance assignments were obtained for 160 of the 181 non-proline S1R residues using a conventional set of TROSY-based experiments (HNCA, HNCACB, CBCA(CO)NH and HNCO) collected with non-uniform sampling (NUS). For NUS, random sampling schedules were used, with typically 15% of the total number of points collected. Spectra were reconstructed with compressed sensing using qMDD [23], processed using NMRPipe [24], and analyzed using NMRView [25]. The assigned chemical shifts have been deposited to the BMRB with accession code 25410.

The secondary structure of S1R(Δ 35) was predicted from backbone ¹H_N, ¹⁵N, ¹³C, ¹³C α and sidechain ¹³C β chemical shifts using TALOS-N [26]. ¹⁵N R₁, R₂ and ¹H–¹⁵N heteronuclear NOE values were measured with TROSY-based sequences collected on a 0.4 mM ¹⁵N, ¹³C-labeled S1R(Δ 35) sample at 600 MHz using the following relaxation delays: 10, 175, 350 and 525 ms (R₁), and 0, 17, 51 and 85 ms (R₂). The recycle delays for R₁, R₂ and heteronuclear NOE experiments were 1.5 s.

3. Results

The S1R(Δ 35) construct contains the cytosolic domain, the region of the second transmembrane domain, and the chaperone domain, but lacks the first transmembrane domain (predicted in residues 9–30) and approximately eight luminal, N-terminal residues. S1R(Δ 35) was reconstituted for NMR studies either from inclusion bodies or from the *Escherichia coli* membranes (Fig. 1A). Well resolved backbone amide NMR spectra of S1R(Δ 35) could be obtained in mixed micelles containing the detergent DPC and relatively small amounts of the lipid DPPC. By contrast, a subset of the resonances for S1R(Δ 35) in DPC alone were weak or missing, indicating conformational exchange. The assigned backbone amide resonances are shown in Fig. 1B. No significant chemical shift differences were observed between reconstituted S1R(Δ 35) purified from membranes or inclusion bodies. The effective size of the protein in DPC micelles was assessed by SEC-MALS and TRACT [27]

Table 1
Sequence-based predictions of S1R transmembrane domains.

Algorithm	TM1 (residues)	TM2 (residues)	Refs.
DAS	12–29	99–107	[34]
HMMTOP	13–37	83–107	[35]
Membrain	8–27	89–108	[36]
MEMSAT-SVM	15–30	91–106	[37]
PHOBIUS	9–30	89–111	[38]
PRED-TMR2	9–30	81–100	[39]
SOSUI	13–34	86–108	[40]
SPOCTOPUS	9–29	88–108	[41]
TMHMM	9–31	89–111 ^a	[42]
TMMOD	12–32	Not predicted	[43]
TMpred	9–28	81–101	[44]

^a TMHMM indicated an increased transmembrane helix probability for these residues, but did not identify it as a transmembrane domain.

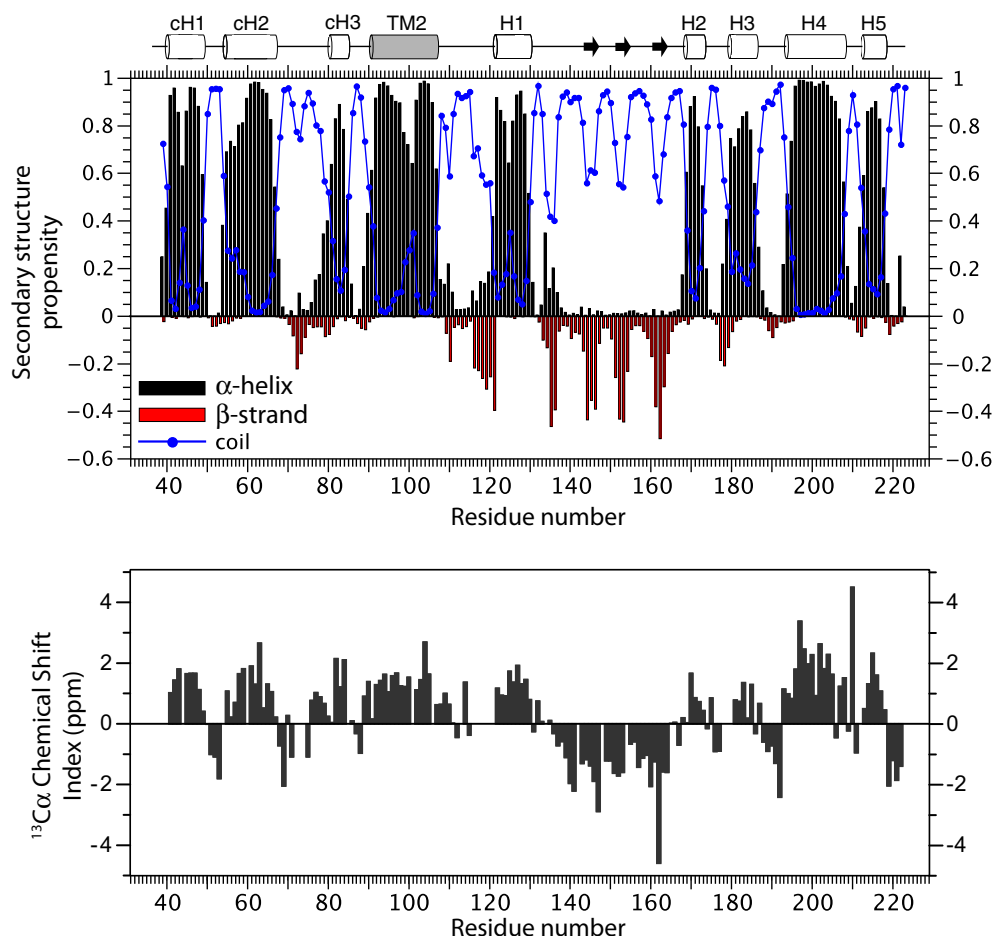


Fig. 2. Chemical shift-based secondary structure analysis of S1R(Δ 35). In the top plot, the TALOS-N [26] outputs are shown, in which the magnitude of the black bars above or red bars below zero on the y-axis indicate the propensities for α -helical or extended conformations, respectively, and the propensities for an unstructured coil conformation are shown as blue circles. In the bottom plot, the $^{13}\text{C}\alpha$ chemical shift index is shown [45]. Above the top plot is shown schematically a summary of the α -helical (cylinders) or extended (arrow) regions.

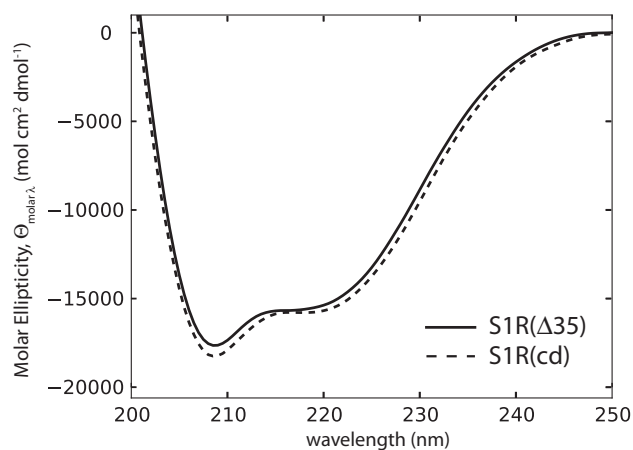


Fig. 3. Far UV circular dichroism spectra of S1R(Δ 35) (continuous line) and S1R(cd) (dashed line) in 50 mM DPC, 5 mM DPPC in 5 mM potassium phosphate, pH 6.5, plotted as the mean residue molar ellipticity per residue.

4. Discussion

S1R functions by regulating a wide range of ion channels and receptors [15]. The activity of S1R itself depends on binding of endogenous and exogenous compounds, and ligand binding has been linked to receptor oligomerisation [18,20]. Possibly reflecting

the diversity of S1R protein–protein interactions, S1R ligands are in clinical use or preclinical studies for a wide variety of diseases [28]. Despite the pharmacological interest in S1R, however, to date structural information has only been available for the C-terminal chaperone domain [21].

Of particular interest is the location and structure of the second transmembrane domain because of its overlap with SBDLI (residues 91–109) [16,17]. Sequence based predictions for TM2 are inconsistent (Table 1), however, predicting either residues ~80–100 or ~90–110, with some predictions being of very low confidence. Glycine residues at positions 87, 88 and 91 have been implicated in ligand binding and receptor oligomerisation [18]. Therefore an accurate definition of TM2 has implications for understanding how these residues participate in ligand binding and possibly also S1R oligomerisation.

We have studied the N-terminal truncation mutant S1R(Δ 35) consisting of all residues from the start of the cytosolic domain through to the chaperone domain, and therefore containing both SBDLI and SBDLII and the glycines at positions 87, 88, and 91. Chemical shift-based secondary structure determination and lipid-induced chemical shift perturbations have been used to infer the location of TM2. Although truncation of the first transmembrane domain or S1R oligomerisation may lead to structural changes, isolated α -helical transmembrane domains solubilized in detergents are known to correlate strongly with that observed in X-ray crystallographic structures of the intact proteins [29]. Our results indicate that the S1R TM2 overlaps nearly completely with

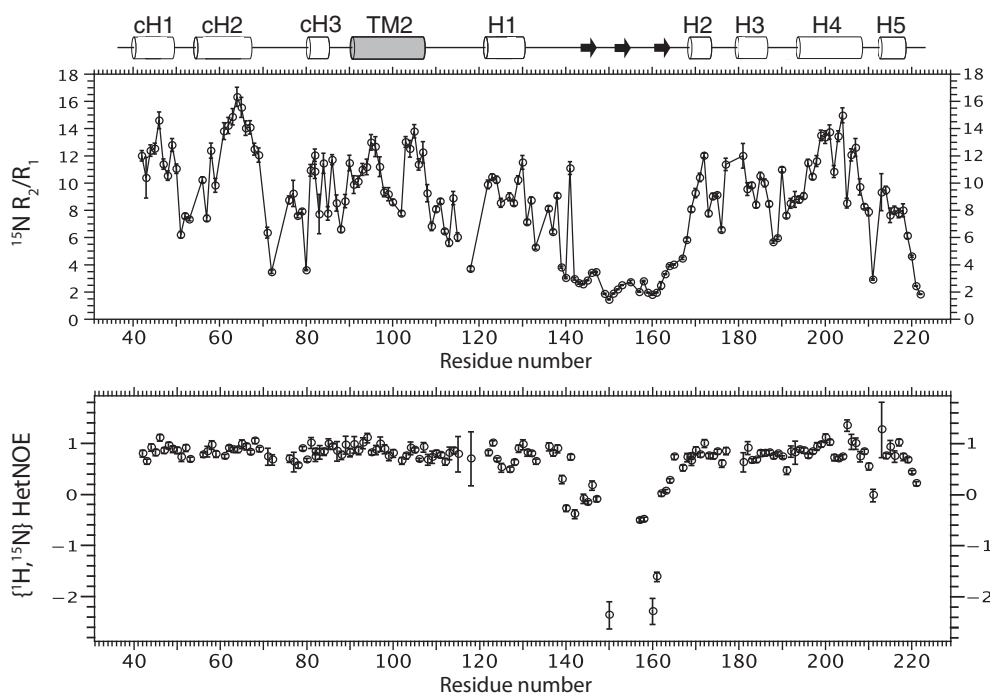


Fig. 4. Dynamic properties of S1R(Δ 35) from relaxation and heteronuclear NOE collected at 600 MHz (^1H) and 41 $^\circ\text{C}$. Top plot: the ratio of the ^{15}N R_2 and R_1 , as a function of residue number for S1R(Δ 35). Bottom plot: the ^1H – ^{15}N heteronuclear NOEs. Residues K142 and S143 exhibited unusually large negative heteronuclear NOEs but were excluded from the plot due to the large uncertainty in the data.

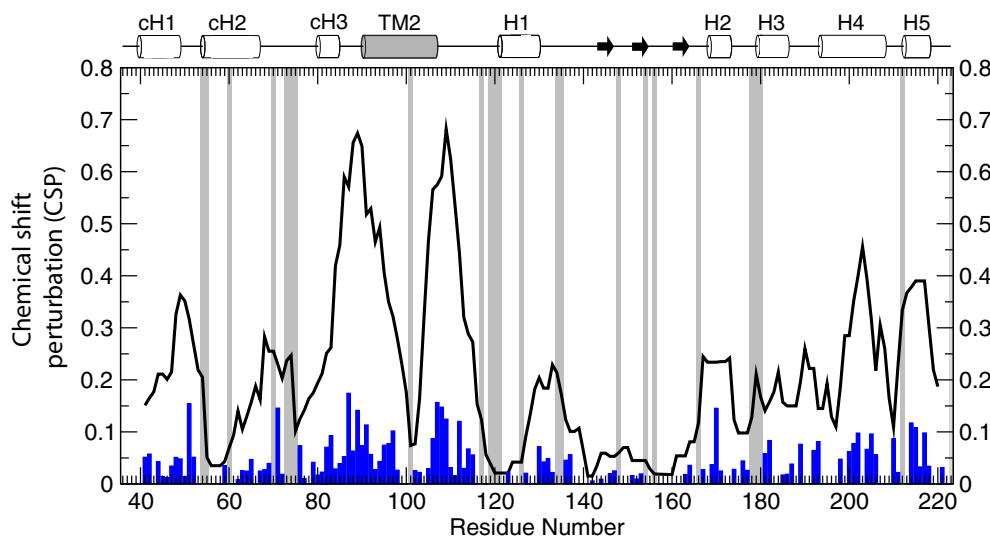


Fig. 5. Chemical shift perturbations in the backbone amide ^1H and ^{15}N resonances of S1R(Δ 35) in DPC upon addition of DPPC to a DPC:DPPC ratio of 1. The solid line indicates the sum of the absolute chemical shift perturbations (CSP) over a 7-residue window, with the magnitude of the CSP for each residue (blue bars) calculated as $\sqrt{\left(\frac{1}{65}\right) \times \Delta\delta_N^2 + (\Delta\delta_H)^2}$. A gray bar indicates prolines or residues for which the chemical shift assignments could not be determined.

SBDLI, and that the adjacent G87 and G88 are not helical. Instead, G87 and G88 are in a linker connecting cH3 to TM2, although they do not exhibit a large increase in flexibility relative to the helical regions. One possibility consistent with these results is that the GGW sequence adopts a structured turn [30].

The position of TM2 determined here is in agreement with the larger subset of transmembrane helix prediction algorithms (in particular, Membrain, MEMSAT-SVM, Phobius, SOSUI, SPOCTOPUS, and TMHMM). The positioning of the helix is also consistent with commonly used non-membrane predictors of α -helices: PSIPRED predicts residues 89–107 to form a helix, and JPRED predicts residues 91–104 to form a helix. However, the positioning is in disagreement with a subset of the tested transmembrane helix

prediction algorithms (Table 1). The lack of consensus in predicting the position of TM2 is likely due to the presence of several polar residues within the transmembrane domain. The center of TM2 is highly amphipathic, with residues 96–104 (“LHASLSEYV”) having a large, hydrophobic moment [31]. Interestingly, several of these residues, including H97 [18], S99 and Y103 [32] have been implicated in drug binding. In addition, the substitution E102Q has been implicated in a form of amyotrophic lateral sclerosis and leads to membrane mislocalisation of S1R in neuronal cells [33].

A comparison of the chaperone domain secondary structure in S1R(Δ 35) with that determined previously for the chaperone domain on its own [21] indicates that the domain structure is largely maintained in the longer S1R(Δ 35) construct. The largest

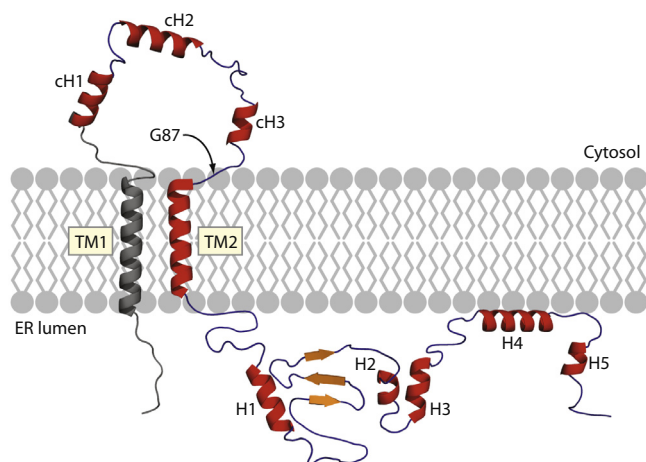


Fig. 6. A schematic diagram of full-length S1R in a lipid bilayer showing the secondary structure determined here for S1R(Δ 35) construct. The loop preceding TM2 contains G87, which is the first residue in the GGWMG sequence, and is indicated with an arrow. SBDLI corresponds closely to TM2 and SBDLII corresponds to H3 and the adjacent coil regions. No experimental data for the first transmembrane domain and N-terminus (colored gray) is available, although the first transmembrane domain is robustly predicted to be composed of the residues from approximately 9 to 30.

changes occur in the C-terminal end of H1, which becomes more dynamic in S1R(Δ 35), and residues 160–164, which have a stronger propensity for an extended conformation in S1R(Δ 35) (Fig. 2). A comparison of the CD spectra for S1R(Δ 35) and S1R(cd) supports a similar proportion of α -helical structure in the two constructs, consistent with that determined from the NMR chemical shifts. In addition, comparison of CD spectra collected in DPC micelles and DPC:DPPC mixed micelles indicated that the helical regions of both S1R(cd) and S1R(Δ 35) are stabilized with the presence of lipid molecules [21].

In conclusion, we have characterized the secondary structure of a construct of S1R missing only the eight residue N-terminus and the first transmembrane domain. Because the first transmembrane helix is robustly predicted (Table 1), a secondary structure schematic of essentially the entire receptor can be made (Fig. 6). The second transmembrane helix, TM2, was found to be composed of residues 91–107, which corresponds closely to the SBDLI. The cytosolic domain contains three α -helices, and the secondary structure of the chaperone domain was largely unchanged by the presence of additional native S1R sequence. The third cytosolic helix (residues 81–85) was mobile compared with cH1 and cH2, and an only modest increase in mobility of the GGW motif that joins cH3 to TM2 was observed. These findings facilitate interpretation of previous results and will guide design of subsequent studies of the role of TM2 in ligand binding and oligomerisation. These results also constitute a significant step toward a complete structure determination of S1R that will lead to a better atomic-level understanding of S1R function.

Acknowledgements

This work was funded by the UK Medical Research Council (K018590) and a FEBS Long-Term Fellowship (J.L.O.R.).

Appendix A. Supplementary data

Supplementary data associated with this article can be found, in the online version, at <http://dx.doi.org/10.1016/j.febslet.2015.01.033>.

References

- [1] Hayashi, T. and Su, T.P. (2007) Sigma-1 receptor chaperones at the ER-mitochondrion interface regulate Ca²⁺ signaling and cell survival. *Cell* 131, 596–610.
- [2] Hayashi, T. and Su, T.P. (2001) Regulating ankyrin dynamics: roles of sigma-1 receptors. *Proc. Natl. Acad. Sci. U.S.A.* 98, 491–496.
- [3] Pal, A., Fontanilla, D., Gopalakrishnan, A., Chae, Y.K., Markley, J.L. and Ruoho, A.E. (2012) The sigma-1 receptor protects against cellular oxidative stress and activates antioxidant response elements. *Eur. J. Pharmacol.* 682, 12–20.
- [4] Wu, Z. and Bowen, W.D. (2008) Role of sigma-1 receptor C-terminal segment in inositol 1,4,5-trisphosphate receptor activation: constitutive enhancement of calcium signaling in MCF-7 tumor cells. *J. Biol. Chem.* 283, 28198–28215.
- [5] Balasuriya, D., D'Sa, L., Talker, R., Dupuis, E., Maurin, F., Martin, P., Borgese, F., Soriani, O. and Edwardson, J.M. (2014) A direct interaction between the sigma-1 receptor and the hERG voltage-gated K⁺ channel revealed by atomic force microscopy and homogeneous time-resolved fluorescence (HTRF(R)). *J. Biol. Chem.* 289, 32353–32363.
- [6] Kourrich, S., Hayashi, T., Chuang, J.Y., Tsai, S.Y., Su, T.P. and Bonci, A. (2013) Dynamic interaction between sigma-1 receptor and Kv1.2 shapes neuronal and behavioral responses to cocaine. *Cell* 152, 236–247.
- [7] Balasuriya, D., Stewart, A.P., Crottes, D., Borgese, F., Soriani, O. and Edwardson, J.M. (2012) The sigma-1 receptor binds to the Nav1.5 voltage-gated Na⁺ channel with 4-fold symmetry. *J. Biol. Chem.* 287, 37021–37029.
- [8] Tchedre, K.T., Huang, R.Q., Dibas, A., Krishnamoorthy, R.R., Dillon, G.H. and Yorio, T. (2008) Sigma-1 receptor regulation of voltage-gated calcium channels involves a direct interaction. *Invest. Ophthalmol. Vis. Sci.* 49, 4993–5002.
- [9] Carnally, S.M., Johannessen, M., Henderson, R.M., Jackson, M.B. and Edwardson, J.M. (2010) Demonstration of a direct interaction between sigma-1 receptors and acid-sensing ion channels. *Biophys. J.* 98, 1182–1191.
- [10] Balasuriya, D., Stewart, A.P. and Edwardson, J.M. (2013) The sigma-1 receptor interacts directly with GluN1 but not GluN2A in the GluN1/GluN2A NMDA receptor. *J. Neurosci.* 33, 18219–18224.
- [11] Navarro, G., Moreno, E., Aymerich, M., Marcellino, D., McCormick, P.J., Mallol, J., Cortes, A., Casado, V., Canela, E.L., Ortiz, J., Fuxe, K., Lluis, C., Ferré, S. and Franco, R. (2010) Direct involvement of sigma-1 receptors in the dopamine D1 receptor-mediated effects of cocaine. *Proc. Natl. Acad. Sci. U.S.A.* 107, 18676–18681.
- [12] Weissman, A.D., Su, T.P., Hedreen, J.C. and London, E.D. (1988) Sigma receptors in post-mortem human brains. *J. Pharmacol. Exp. Ther.* 247, 29–33.
- [13] Seth, P., Ganapathy, M.E., Conway, S.J., Bridges, C.D., Smith, S.B., Casellas, P. and Ganapathy, V. (2001) Expression pattern of the type I sigma receptor in the brain and identity of critical anionic amino acid residues in the ligand-binding domain of the receptor. *Biochim. Biophys. Acta* 1540, 59–67.
- [14] Maurice, T. and Su, T.P. (2009) The pharmacology of sigma-1 receptors. *Pharmacol. Ther.* 124, 195–206.
- [15] Kourrich, S., Su, T.P., Fujimoto, M. and Bonci, A. (2012) The sigma-1 receptor: roles in neuronal plasticity and disease. *Trends Neurosci.* 35, 762–771.
- [16] Pal, A., Hajipour, A.R., Fontanilla, D., Ramachandran, S., Chu, U.B., Mavlyutov, T. and Ruoho, A.E. (2007) Identification of regions of the sigma-1 receptor ligand binding site using a novel photoprobe. *Mol. Pharmacol.* 72, 921–933.
- [17] Pal, A., Chu, U.B., Ramachandran, S., Grawoig, D., Guo, L.W., Hajipour, A.R. and Ruoho, A.E. (2008) Juxtaposition of the steroid binding domain-like I and II regions constitutes a ligand binding site in the sigma-1 receptor. *J. Biol. Chem.* 283, 19646–19656.
- [18] Gromek, K.A., Suchy, F.P., Meddaugh, H.R., Wrobel, R.L., LaPointe, L.M., Chu, U.B., Primm, J.G., Ruoho, A.E., Senes, A. and Fox, B.G. (2014) The oligomeric states of the purified sigma-1 receptor are stabilized by ligands. *J. Biol. Chem.* 289, 20333–20344.
- [19] MacKenzie, K.R., Prestegard, J.H. and Engelman, D.M. (1997) A transmembrane helix dimer: structure and implications. *Science* 276, 131–133.
- [20] Chu, U.B., Ramachandran, S., Hajipour, A.R. and Ruoho, A.E. (2013) Photoaffinity labeling of the sigma-1 receptor with N-[3-(4-nitrophenyl)propyl]-N-dodecylamine: evidence of receptor dimers. *Biochemistry* 52, 859–868.
- [21] Ortega-Roldan, J.L., Ossa, F. and Schnell, J.R. (2013) Characterization of the human sigma-1 receptor chaperone domain structure and binding immunoglobulin protein (BiP) interactions. *J. Biol. Chem.* 288, 21448–21457.
- [22] Savitzky, A. and Golay, M.J.E. (1964) Smoothing and differentiation of data by simplified least squares procedures. *Anal. Chem.* 36, 1627–1639.
- [23] Kazimierczuk, K. and Orekhov, V.Y. (2011) Accelerated NMR spectroscopy by using compressed sensing. *Angew Chem-Int Edit* 50 (24), 5556–5559.
- [24] Delaglio, F., Grzesiek, S., Vuister, G.W., Zhu, G., Pfeifer, J. and Bax, A. (1995) NMRPipe: a multidimensional spectral processing system based on UNIX pipes. *J. Biomol. NMR* 6, 277–293.
- [25] Johnson, B.A. (2004) Using NMRView to visualize and analyze the NMR spectra of macromolecules. *Methods Mol. Biol.* 278, 313–352.
- [26] Shen, Y. and Bax, A. (2013) Protein backbone and sidechain torsion angles predicted from NMR chemical shifts using artificial neural networks. *J. Biomol. NMR* 56, 227–241.
- [27] Lee, D., Hilty, C., Wider, G. and Wuthrich, K. (2006) Effective rotational correlation times of proteins from NMR relaxation interference. *J. Magn. Reson.* 178, 72–76.
- [28] Hayashi, T.I., Tsai, S.Y., Mori, T., Fujimoto, M. and Su, T.P. (2011) Targeting ligand-operated chaperone sigma-1 receptors in the treatment of neuropsychiatric disorders. *Expert Opin Ther Targets* 15 (5), 557–577.

- [29] Tulumello, D.V. and Deber, C.M. (2012) Efficiency of detergents at maintaining membrane protein structures in their biologically relevant forms. *Biochim. Biophys. Acta* 1818, 1351–1358.
- [30] Lorieau, J.L., Louis, J.M. and Bax, A. (2011) Helical hairpin structure of influenza hemagglutinin fusion peptide stabilized by charge–dipole interactions between the N-terminal amino group and the second helix. *J. Am. Chem. Soc.* 133, 2824–2827.
- [31] Gautier, R., Douguet, D., Antonny, B. and Drin, G. (2008) HELIQUEST: a web server to screen sequences with specific alpha-helical properties. *Bioinformatics* 24, 2101–2102.
- [32] Yamamoto, H., Miura, R., Yamamoto, T., Shinohara, K., Watanabe, M., Okuyama, S., Nakazato, A. and Nukada, T. (1999) Amino acid residues in the transmembrane domain of the type 1 sigma receptor critical for ligand binding. *FEBS Lett.* 445, 19–22.
- [33] Al-Saif, A., Al-Mohanna, F. and Bohlega, S. (2011) A mutation in sigma-1 receptor causes juvenile amyotrophic lateral sclerosis. *Ann. Neurol.* 70, 913–919.
- [34] Cserzo, M., Wallin, E., Simon, I., von Heijne, G. and Elofsson, A. (1997) Prediction of transmembrane alpha-helices in prokaryotic membrane proteins: the dense alignment surface method. *Protein Eng.* 10, 673–676.
- [35] Tusnady, G.E. and Simon, I. (2001) The HMMTOP transmembrane topology prediction server. *Bioinformatics* 17, 849–850.
- [36] Shen, H. and Chou, J.J. (2008) MemBrain: improving the accuracy of predicting transmembrane helices. *PLoS ONE* 3, e2399.
- [37] Jones, D.T. (2007) Improving the accuracy of transmembrane protein topology prediction using evolutionary information. *Bioinformatics* 23, 538–544.
- [38] Kall, L., Krogh, A. and Sonnhammer, E.L. (2004) A combined transmembrane topology and signal peptide prediction method. *J. Mol. Biol.* 338, 1027–1036.
- [39] Pasquier, C. and Hamodrakas, S.J. (1999) An hierarchical artificial neural network system for the classification of transmembrane proteins. *Protein Eng.* 12, 631–634.
- [40] Hirokawa, T., Boon-Chieng, S. and Mitaku, S. (1998) SOSUI: classification and secondary structure prediction system for membrane proteins. *Bioinformatics* 14, 378–379.
- [41] Viklund, H., Bernsel, A., Skwark, M. and Elofsson, A. (2008) SPOCTOPUS: a combined predictor of signal peptides and membrane protein topology. *Bioinformatics* 24, 2928–2929.
- [42] Krogh, A., Larsson, B., von Heijne, G. and Sonnhammer, E.L. (2001) Predicting transmembrane protein topology with a hidden Markov model: application to complete genomes. *J. Mol. Biol.* 305, 567–580.
- [43] Karsay, R.Y., Gao, G. and Liao, L. (2005) An improved hidden Markov model for transmembrane protein detection and topology prediction and its applications to complete genomes. *Bioinformatics* 21, 1853–1858.
- [44] Hoffmann, K. and Stoffel, W. (1993) TMbase – a database of membrane spanning proteins segments. *Biol. Chem.* 374, 166.
- [45] Spera, S. and Bax, A. (1991) Empirical correlation between protein backbone conformation and C α and C β 13C nuclear magnetic resonance chemical shifts. *J. Am. Chem. Soc.* 113, 5490–5492.